Atomistic modeling of water infiltration in defective zeolite for thermal storage applications

ASME-ATI-UIT 2015 Conference on Thermal Energy Systems: Production, Storage, Utilization and the Environment
17 - 20 May, 2015, Napoli, Italy

ATOMISTIC MODELING OF WATER INFILTRATION IN DEFECTIVE ZEOLITE FOR THERMAL STORAGE APPLICATIONS

Matteo Fasano*, Alessio Bevilacqua**, Eliodoro Chiavazzo***, Pietro Asinari*****

*Energy Department, Politecnico di Torino, Corso Duca degli Abruzzi 24, Turin, 10129, IT. E-mail: matteo.fasano@polito.it
**Energy Department, Politecnico di Torino, Corso Duca degli Abruzzi 24, Turin, 10129, IT. E-mail: alessio.bevilacqua@studenti.polito.it
***Energy Department, Politecnico di Torino, Corso Duca degli Abruzzi 24, Turin, 10129, IT. E-mail: eliodoro.chiavazzo@polito.it
****Energy Department, Politecnico di Torino, Corso Duca degli Abruzzi 24, Turin, 10129, IT. E-mail: pietro.asinari@polito.it

ABSTRACT

In this article, the impact that zeolite materials may have in the near future in *loss-free*, more compact and efficient thermal storage systems is numerically investigated. Water infiltration within MFI zeolite presenting different concentrations of hydrophilic defects is studied by Molecular Dynamics (MD) simulations. Results show that the characteristic infiltration pressure of water in the considered zeolite framework is reduced with increased hydrophilicity. Dubinin-Astakhov model is then applied to link zeolite-water interaction energy with the resulting infiltration isotherms of the nanoporous material. The effort, therefore, is to gather some model-driven guidelines towards innovative materials for thermal systems that may be manufactured and employed in the near future for addressing a great challenge of our society: storage and use of thermal energy.

Keywords: *Zeolite, Thermal storage, Water, Microporous materials, Molecular dynamics*

INTRODUCTION

In the last decades, the increase in worldwide human population, industrialization and technological development have been causing a growth in the usage of fossil fuels, which in turn has increased greenhouse gas emissions and fuel prices [1]. The latter events contributed to the diffusion of novel solutions for the exploitation of various renewable energy resources, such as solar, tidal, wind or geothermal technologies [2]. One of the major bottlenecks that is currently limiting a more extensive diffusion of the latter technologies is the mismatch between most renewable energy supplies and user demand, which is particularly the case of solar energy due to its intrinsically intermittent and unpredictable nature [1; 3; 4]. Therefore, energy storage systems are an appropriate way to provide equilibrium between energy supply and demand, with the aim to make accessible everywhere and every time the electrical and thermal energies produced when and where renewable sources are available, at least at the regional scale.

Sensible [5] or latent [6] heat storage systems are the most studied and developed solutions in this field; however, the latter methods are not suitable for long-term storage, being susceptible to a progressive loss of thermal energy [7]. On the contrary, storage systems based on sorption phenomena show high energy density, negligible heat losses and allow repetitive storage operations [8]. In this context, zeolite materials are showing great potential for heat storage applications.

Zeolites are aluminosilicate materials that can be easily synthesized with a precise chemical composition and structure of the micropores [9]. The significant increase in the surface to volume ratio and the peculiar physical properties of water under nanoconfined conditions are the main motivations of the growing interest for zeolite materials in several fields [10; 11; 12]. In fact, the increased solvent accessible surface enhances the solid-liquid interactions, which in turn modify the liquid transport properties due to nanoconfinement effects. Such effects can be exploited to tailor and improve performances of thermal storage devices, desalinators, molecular sieves or catalysts [13].

In particular, zeolites present both large heat of adsorption and the capability to adsorb/desorb water molecules without significant structure degradation, thus allowing durable heat release/accumulation cycles, respectively [14; 15]. Other advantages of zeolite materials are the non-toxicity and the low mass density [16], which make them ideal materials for sorption heat storage systems for both heating [17; 18] and cooling purposes [19]. However, while the nanometer size of zeolite's pores allows the sorption process to take place with large surface to volume ratios (e.g. as a rule of thumb, a teaspoon of zeolite or MOF materials have a inner pore surface equal to the area of a football field [20]) thus with high energy densities, it also involves non-trivial nanoscale effects on the mass transport of water inside the nanopores, such as surface barriers, single-file diffusion and nanoconfinement [21; 22; 23; 24].

Therefore, a lack of understanding of the mechanisms governing the water transport in their nanoporous matrix as well as a challenging control of the synthesis process are currently limiting the commercialization of zeolite-based thermal storage applications. Mass transport of water in the nanoporous matrix of zeolite is determined by geometric (i.e. pore size and network), physical (i.e. pore filling, temperature, pressure) and chemical (i.e. solid-liquid nonbonded interactions) factors [23]. In particular, the affinity (i.e. hydrophilicity degree) between the zeolite matrix and water can be controlled by introducing hydrophilic defects in a pristine hydrophobic framework, thus precisely tuning the equilibrium and non-equilibrium mass transfer properties of the intruded water. For example, pristine MFI-type zeolite (also known as silicalite-1) shows hydrophobic behavior; however, aluminum defects can be introduced in

*Corresponding author

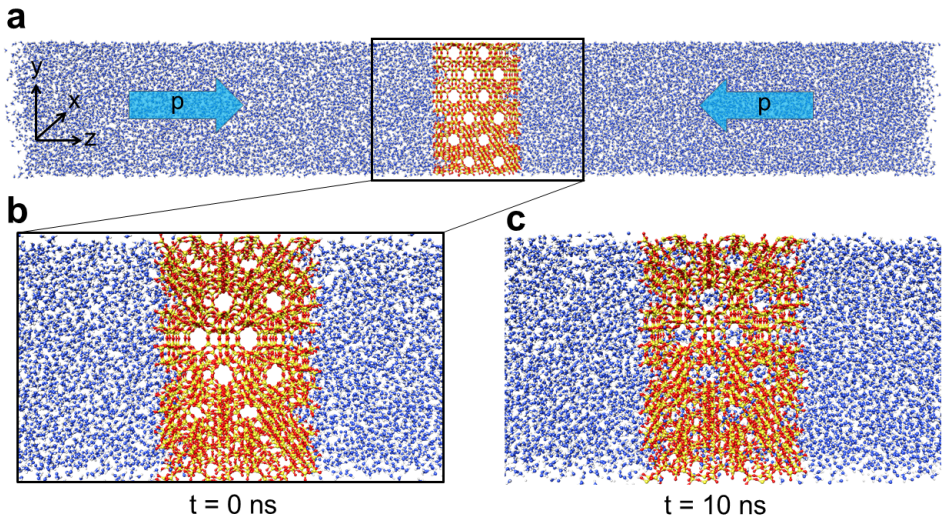

Figure 1. Simulated MD configuration. (a) Schematics of the MD simulation box: MFI zeolite membrane (red/yellow) and water molecules (blue) are represented. (b) MFI zeolite membrane before the water infiltration. (c) MFI zeolite membrane completely infiltrated, after 10 ns of simulation with p solvent pressure.

the pristine structure without affecting the pore size. Aluminum defects foster the creation of silanols (i.e. SiOH) thus a progressive increase of the hydrophilicity of the nanoporous framework [25]. While hydrophilic pores enhance the water uptake at adsorption and infiltration pressures [25; 26], some recent experimental studies have shown a significant increase in the transport of water in nanometer-sized hydrophobic pores [25]. Hence, since the permeability of a porous material is dependent on both equilibrium (solubility, namely the sorption coefficient) and non-equilibrium (diffusivity) transport properties, it is unclear which property is dominant in controlling the overall transport behavior [25].

The experimental investigation of the peculiar behavior of water within the zeolites is often limited by fabrication and visualization techniques; however, atomistic simulations can help to investigate transport properties of water under such nanoconfined conditions [12; 26]. Hence, silicalite-1 is the ideal platform for studying water transport within nanopores characterized by increasing degrees of hydrophilicity; whereas Molecular Dynamics (MD) simulations can be used to evaluate both equilibrium (i.e. infiltration isotherms) and non-equilibrium (i.e. transport diffusion) water properties under such nanoconfined conditions.

In this work, MD is used to study the mechanism of water infiltration in defective MFI zeolites, in order to suggest guidelines for a more rational design of novel nanoporous materials with tailored water infiltration properties for heat storage applications.

METHODS

The simulated MD setup is designed for estimating the equilibrium water filling of a x,y periodic membrane at different solvent pressures, which allows obtaining the characteristic water infiltration isotherm of the tested material. The membrane is made out of pristine or defective silicalite-1 (2x3x3 crystal cells) and it is restrained in the center of the simulation box. The membrane is then solvated in a large water box (about 30000 molecules are typically added, see Fig. 1a), whereas the water-zeolite interface normal to z axis is functionalized by silanol terminals.

The force field adopted in the MD simulations takes into account both bonded and nonbonded interactions. Bonded interactions in the MFI crystal are modeled by both stretch and angle harmonic potentials. Parameters of the bonded interactions are reported elsewhere [27]. Nonbonded interactions between zeolite and water are crucial for defining the adsorption/infiltration characteristics of the studied material [26; 28]. Here, van der Waals interactions are modeled by a 12-6 Lennard-Jones (LJ) potential; partial charge interactions between solid surfaces and water are modeled by a Coulomb potential. Initially, both LJ and partial charges of MFI zeolite are taken from the values reported by Cailliez *et al.* [26], where partial charges of silicon, oxygen and hydrogen atoms in the MFI structure are $q_{Si} = 1.4$ e, $q_O = -q_{Si}/2$ and $q_H = q_{Si}/4$, respectively. The value of q_{Si} is successively tuned in order to better mimic experimental infiltration isotherms. TIP4P water model is adopted for the solvent [29], because it well reproduces the transport properties of water molecules confined in MFI zeolite [26]. Intramolecular interactions of water molecules are fixed by LINCS algorithm [30], in order to increase the simulation timestep.

After that geometry is energy minimized, system velocities are initialized by a Maxwell distribution (300 K). System temperature is then equilibrated at 300 K and water pressure stabilized around 0.1 MPa by successive NVT and NPT runs, where Berendsen thermostat and barostat are used. Finally, infiltration runs are performed in NPT ensemble (velocity rescaled Berendsen thermostat with T=300 K; isotropic Parrinello-Rahman barostat with p water pressure to be tested), so that water molecules can intrude in the initially empty zeolite membrane (Fig. 1b) until equilibrium conditions are reached (Fig. 1c), typically after 10–35 ns. *In silico* infiltration experiments are performed in the pressure range 25-250 MPa, and only water molecules in the central portion of the membrane are considered as infiltrated, in order to avoid artifacts due to the broken crystallinity at the solid-liquid interface. Up to three repetitions per simulation with different initial conditions are performed and results averaged, for better statistics. Steady state is considered as achieved when the water uptake ω, which is the average amount of water molecules infiltrated per MFI unit cell

(N/UC), converges to a constant value (Fig. 2). The latter corresponds to the amount of water molecules in thermodynamic equilibrium with the system's chemical potential (i.e. pressure). Kinetic end potential energies as well as pressure are checked for convergence during the simulation.

MD simulations are carried out by means of GROMACS [31] software, while rendering pictures are made with UCSF Chimera [32]. Lennard-Jones potentials are treated with a twin-range cut-off modified by a shift function (1.0 nm cut-off distance), whereas the Particle-Mesh Ewald (PME) algorithm [33] with 1 nm real-space cutoff and 0.12 nm reciprocal space gridding is chosen for electrostatic interactions. Simulations are performed with a leap-from algorithm and time step $\Delta t = 2$ fs. Long range dispersion corrections are applied to avoid energy artifacts.

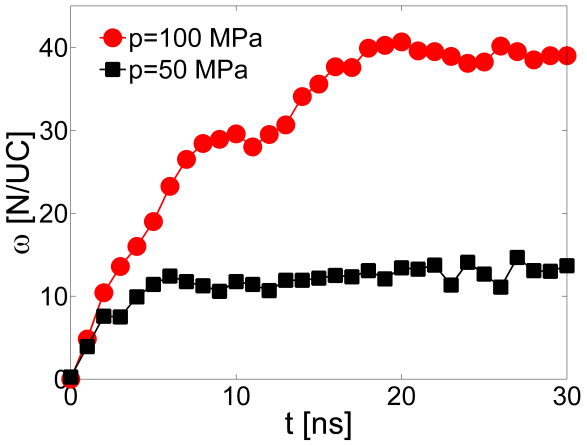

Figure 2. Water uptake ω in a MFI membrane with 0.89% Al/Si defect concentrations, with p =50 (black squares) or 100 (red circles) MPa.

RESULTS

First, the infiltration isotherm of water in silicalite-1 obtained from MD simulations is compared with the experimental results presented in Reference [9]. Partial charges of the zeolite structure are then tuned for mimicking the experimental infiltration pressure ($\cong$ 100 MPa [9]): starting from the value suggested by Caillez *et al.* ($q_{Si} = 1.4$ e), MD runs show that q_{Si}=1.8 e better reproduces the experimental infiltration pressure of silicalite-1 (Fig. 3).

Note that the maximum framework infiltration capacity (ω_M) of the simulated structure is larger than the experimental evidence reported by Humplik *et al.*, namely 52 N/UC vs. 35 N/UC, respectively [9]. However, similar values have been found in other experimental (i.e. 53 N/UC [34]) and numerical studies (i.e. 57 N/UC [35]). The latter discrepancy with experiments may be due to the analysis of imperfect zeolite specimens, which may present surface barriers, pore blockage or contamination of the structure thus modifications of the accessible pore volume. On the other hand, numerical results may be affected by not optimized force field parameters, such as water model or Lennard-Jones coefficients. For the sake of completeness, while water model is kept constant in the following simulations, the effect of Lennard-Jones parameters on ω_M has been investigated. In particular, the inter-particle distance at which the LJ potential is zero for the oxygen atoms of the MFI zeolite

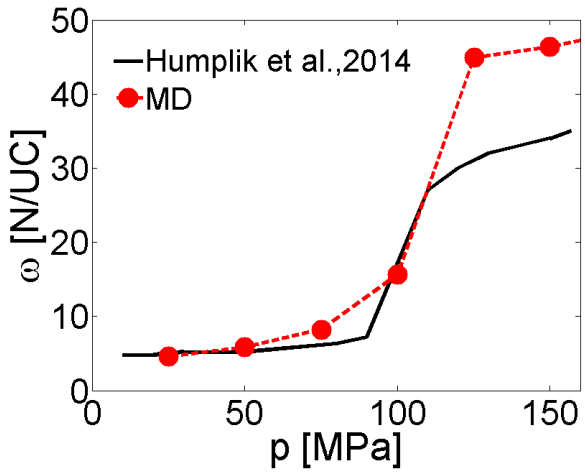

Figure 3. Infiltration isotherm of water in a silicalite-1 membrane. Results from current MD simulations (red dots and red dashed line) are compared with the experimental ones reported by Humplik *et al.* (black line) [25].

is varied (σ). Starting from the base case (i.e. $\sigma = 0.30$ nm [26]), σ is increased up to 0.42 nm and the water uptake ω_M at $p = 250$ MPa evaluated by MD simulations. Considering a silicalite-1 membrane, Fig. 4 shows that ω_M decreases as σ increases. Therefore, the ω_M decrease is due to the reduction of water accessible volume in the zeolite's nanopores. However, changes in ω_M do not affect the dependence between infiltration pressures (i.e. infiltration type) and structure hydrophilicity [25], which is the focus of the following analysis.

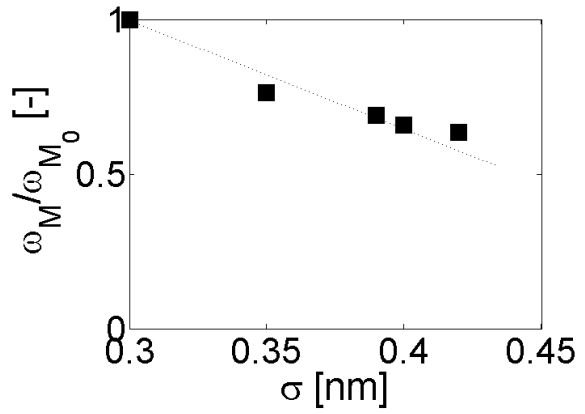

Figure 4. Influence of σ Lennard-Jones parameter for the oxygen atoms of silicalite-1 membrane on the maximum framework infiltration capacity ω_M. Results are scaled by the framework capacity ω_{M0} of the base case, namely the case with $\sigma = 0.30$ nm. The black dotted line is a linear fitting of MD results.

After the preliminary tuning of the zeolite force field on experimental results, hydrophilic defects are introduced in the pristine structure, in order to study the infiltration behavior of water in MFI membranes with different hydrophilicity. Here, defects mimic the substitution of silicon atoms by aluminum ones, which induces the creation of four local silanol nests [26]. Setups with increasing densities of randomly distributed defects are tested, namely MFI with either 0.89% or 3.06% Al substitutions respect to the total amount of Si atoms in the structure

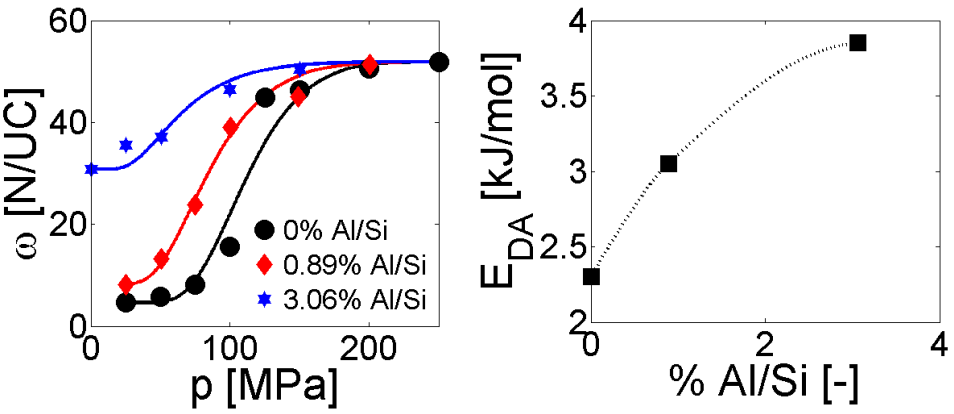

Figure 5. Infiltration isotherms of water in defected MFI zeolites and D-A interpretation. (a) Infiltration isotherms of water in MFI zeolites with different defect densities: MD results (dots) vs. D-A model (solid lines). (b) D-A energy parameter (E_{DA} in Eq. 1) at different defect densities.

(%Al/Si).

Results in Figure 5a show that small increases in the defect concentration (i.e. structure hydrophilicity) induce both a significant shift of the infiltration pressures toward lower values (e.g. approximately from 100 MPa for pristine silicalite-1 to 70 MPa by introducing 0.89% Al substitutions) and the change of the infiltration isotherm shape (i.e. from type-V to type-I), coherently with experimental evidences and previous modeling works [25; 26].

A relation between the obtained infiltration isotherms and the geometrical, physical and chemical characteristics of the membrane is needed for a better comprehension of the infiltration phenomena. Dubinin-Astakhov model (D-A) has been widely adopted for interpreting the dynamics of adsorption-infiltration processes [36]. In the followings, the obtained numerical infiltration isotherms are fitted by D-A model, which allows to interpret the results with a minimal number of physical parameters, namely:

$$\frac{\omega-\omega_m}{\omega_M-\omega_m}=\exp\left[-\left(\frac{-k_B N_A T}{E_{DA}}\ln\frac{p}{p_M}\right)^{n_{DA}}\right], \qquad (1)$$

where ω_m and ω_M are adsorption and infiltration maximum framework capacities, respectively; p_M is the pressure at which ω_M is reached; E_{DA} and n_{DA} are D-A parameters related to the water-structure interaction energy and structure geometry, respectively; k_B is the Boltzmann constant, N_A the Avogadro number and T the system temperature. While ω_m, ω_M and p_M are known quantities, E_{DA} and n_{DA} are fitted to MD results. Here, the zeolite structure is assumed as invariant in the simulated setups thus n_{DA} constant, whereas E_{DA} related to the defect densities. By means of optimizations based on genetic algorithm, $n_{DA}=3.14$ is found to be the most accurate D-A exponent for the simulated MFI membranes, whereas the optimized E_{DA} values for different defect concentrations are presented in Figure 5b. Figure 5b shows that D-A model (Eq. 1) accurately fits ($R^2>0.90$) the obtained MD infiltration isotherms. As expected, the energy parameter E_{DA} increases with defect concentration, because the larger amount of hydrophilic spots in the structure implies higher interaction energies between the membrane and the intruded water molecules. E_{DA} values seem to saturate while approaching large defect densities, which means that the infiltration behavior of water becomes mostly governed by defect-liquid interactions rather than framework-liquid ones. Note that ω_M is independent from defect concentration, because it is only determined by the solvent accessible volume of the nanoporous structure.

Therefore, a few physical considerations about the infiltration phenomena occurring with different structure hydrophilicity can be formulated. First, infiltration isotherms are clearly type-V at low defect concentrations (i.e. less than 1% Al/Si), which means that the membrane has an overall hydrophobic behavior. In this case, no infiltration occurs at low pressures, because bulk liquid-liquid interactions are stronger than the solid-liquid ones. Therefore, water condensation is dominated by liquid-liquid interactions at the infiltration pressure. In fact, the condensation process starts with the homogeneous nucleation of water molecules and it is then followed by the collapse of the latter water clusters into the bulk liquid phase at the infiltration pressure [26; 28; 37]. Second, defect concentrations larger than 1% Al/Si progressively transform infiltration isotherms from type-V to type-I shape. In this case, on the contrary, solid-liquid interactions become dominant in the condensation process, thus inducing a heterogeneous nucleation of water molecules in the proximity of the most hydrophilic (i.e. defected) regions of the membrane [26; 34; 38; 39].

CONCLUSIONS

In this article, the infiltration behavior of water in zeolite membranes, which are promising materials for thermal storage applications, are analyzed by molecular dynamics. The introduction of hydrophilic defects in a hydrophobic nanoporous material is the approach suggested for controlling the characteristic infiltration isotherms. Starting from a hydrophobic structure (i.e. silicalite-1), the hydrophilicity of the zeolite membrane is then tuned by defect concentration.

Numerical infiltration isotherms are interpreted by D-A model with a minimal number of physical parameters, namely n_{DA} and E_{DA} (Eq. 1). While n_{DA} may be related to the crystal structure, E_{DA} takes into account the water-zeolite interactions. Results show that E_{DA} is enhanced by increased hydrophilicity, namely larger defect concentration. Furthermore, these numerical results demonstrate that small concentration of hydrophilic defects can significantly alter the infiltration characteristics of hydrophobic nanoporous materials, as also experimentally observed by Humplik and colleagues [25].

In conclusion, the interaction energy between intruded water and MFI zeolites is a fundamental quantity for understand-

ing their characteristic water infiltration behavior. Water-zeolite interactions are increased by introducing defects in the pristine (hydrophobic) structure, namely by increasing the density of inner hydrophilic spots. The latter findings may guide the design of next generation highly permeable materials for thermal storage applications.

ACKNOWLEDGMENT

Authors are grateful to MITOR project (Compagnia di Sanpaolo) for travel support. PA, EC and MF would like to acknowledge the THERMALSKIN project for the revolutionary surface coatings by carbon nanotubes for high heat transfer efficiency (FIRB 2010, grant number RBFR10VZUG) and the NANO-BRIDGE project for the heat and mass transport in NANO-structures by molecular dynamics, systematic model reduction, and non-equilibrium thermodynamics (PRIN 2012, grant number 2012LHPSJC). MF acknowledges travel support from the Scuola Interpolitecnica di Dottorato - SCUDO. Authors thank the CINECA (Iscra C project DISCALIN) and the Politecnico di Torino (DAUIN) high-performance computing initiative for the availability of high-performance computing resources and support. Authors are grateful to Dr. Thomas Humplik and Prof. Evelyn Wang (MIT) for the valuable discussions.

REFERENCES

[1] K. E. N'Tsoukpoe, H. Liu, N. Le Pierres, and L. Luo, "A review on long-term sorption solar energy storage," *Renewable and Sustainable Energy Reviews*, vol. 13, no. 9, pp. 2385–2396, 2009.

[2] D. Aydin, S. P. Casey, and S. Riffat, "The latest advancements on thermochemical heat storage systems," *Renewable and Sustainable Energy Reviews*, vol. 41, pp. 356–367, 2015.

[3] H. Garg, S. Mullick, and A. Bhargava, *Solar thermal energy storage*. Springer, 1985.

[4] F. Kreith and J. F. Kreider, "Principles of solar engineering," *Washington, DC, Hemisphere Publishing Corp., 1978. 790 p.*, vol. 1, 1978.

[5] K. Nielsen, "Thermal energy storage: A state-of-the-art," *Norway: Department of Geology and Mineral Resources Engineering, Trondheim*, p. 25, 2003.

[6] B. Zalba, J. M. Marín, L. F. Cabeza, and H. Mehling, "Review on thermal energy storage with phase change: materials, heat transfer analysis and applications," *Applied thermal engineering*, vol. 23, no. 3, pp. 251–283, 2003.

[7] Y. Kato, "Chemical energy conversion technologies for efficient energy use," in *Thermal energy storage for sustainable energy consumption*, pp. 377–391, Springer, 2007.

[8] A. Hauer, "Sorption theory for thermal energy storage," in *Thermal energy storage for sustainable energy consumption*, pp. 393–408, Springer, 2007.

[9] T. Humplik, R. Raj, S. C. Maroo, T. Laoui, and E. N. Wang, "Framework water capacity and infiltration pressure of MFI zeolites," *Microporous and Mesoporous Materials*, vol. 190, pp. 84–91, 2014.

[10] T. Humplik, J. Lee, S. O'Hern, B. Fellman, M. Baig, S. Hassan, M. Atieh, F. Rahman, T. Laoui, R. Karnik, *et al.*, "Nanostructured materials for water desalination," *Nanotechnology*, vol. 22, no. 29, p. 292001, 2011.

[11] A. Bertucci, H. Lulf, D. Septiadi, A. Manicardi, R. Corradini, and L. De Cola, "Intracellular delivery of peptide nucleic acid and organic molecules using zeolite-l nanocrystals," *Advanced healthcare materials*, 2014.

[12] E. Chiavazzo, M. Fasano, P. Asinari, and P. Decuzzi, "Scaling behaviour for the water transport in nanoconfined geometries," *Nature communications*, vol. 5, p. 4495, 2014.

[13] M. Fasano, E. Chiavazzo, and P. Asinari, "Water transport control in carbon nanotube arrays," *Nanoscale research letters*, vol. 9, no. 1, pp. 1–8, 2014.

[14] J. Janchen, D. Ackermann, H. Stach, and W. Brosicke, "Studies of the water adsorption on zeolites and modified mesoporous materials for seasonal storage of solar heat," *Solar Energy*, vol. 76, no. 1-3, pp. 339–344, 2004.

[15] M. Fasano, M. B. Bigdeli, M. R. Sereshk Vaziri, E. Chiavazzo, and P. Asinari, "Thermal transmittance of carbon nanotube networks: Guidelines for novel thermal storage systems and polymeric material of thermal interest," *Renewable & Sustainable Energy Reviews*, vol. 41, pp. 1028–1036, 2015.

[16] R. A. Shigeishi, C. H. Langford, and B. R. Hollebone, "Solar energy storage using chemical potential changes associated with drying of zeolites," *Solar Energy*, vol. 23, no. 6, pp. 489–495, 1979.

[17] C. F. Parrish, R. P. Scaringe, and D. M. Pratt, "Development of an innovative spacecraft thermal storage device," in *IECEC'91; Proceedings of the 26th Intersociety Energy Conversion Engineering Conference, Volume 4*, vol. 4, pp. 279–284, 1991.

[18] A. Hauer, "Thermal energy storage with zeolite for heating and cooling applications," in *Proceedings of 3rd Workshop of Annex*, vol. 17, pp. 1–2, 2002.

[19] Y. Lu, R. Wang, M. Zhang, and S. Jiangzhou, "Adsorption cold storage system with zeolite–water working pair used for locomotive air conditioning," *Energy conversion and management*, vol. 44, no. 10, pp. 1733–1743, 2003.

[20] K. Sanderson, "Materials chemistry: Space invaders," *Nature*, vol. 448, no. 7155, pp. 746–748, 2007.

[21] J. Kärger, "In-depth study of surface resistances in nanoporous materials by microscopic diffusion measurement," *Microporous and Mesoporous Materials*, 2013.

[22] J. Kärger, T. Binder, C. Chmelik, F. Hibbe, H. Krautscheid, R. Krishna, and J. Weitkamp, "Microimaging of transient guest profiles to monitor mass transfer in nanoporous materials," *Nature Materials*, vol. 13, no. 4, pp. 333–343, 2014.

[23] R. Taylor and R. Krishna, *Multicomponent mass transfer*, vol. 597. Wiley New York, 1993.

[24] R. Krishna, "Diffusion in porous crystalline materials," *Chemical Society Reviews*, vol. 41, no. 8, pp. 3099–3118, 2012.

[25] T. Humplik, R. Raj, S. Maroo, T. Laoui, and E. N. Wang, "Effect of hydrophilic defects on water transport in MFI zeolites," *Langmuir*, vol. 30, no. 22, pp. 6446–6453, 2014.

[26] F. Cailliez, G. Stirnemann, A. Boutin, I. Demachy, and A. H. Fuchs, "Does water condense in hydrophobic cavities? a molecular simulation study of hydration in heterogeneous nanopores," *The Journal of Physical Chemistry C*, vol. 112, no. 28, pp. 10435–10445, 2008.

[27] P. E. Lopes, V. Murashov, M. Tazi, E. Demchuk, and A. D. MacKerell, "Development of an empirical force field for silica. application to the quartz-water interface," *The Journal of Physical Chemistry B*, vol. 110, no. 6, pp. 2782–

2792, 2006.

[28] N. Desbiens, A. Boutin, and I. Demachy, "Water condensation in hydrophobic silicalite-1 zeolite: A molecular simulation study," *The Journal of Physical Chemistry B*, vol. 109, no. 50, pp. 24071–24076, 2005.

[29] W. L. Jorgensen, J. Chandrasekhar, J. D. Madura, R. W. Impey, and M. L. Klein, "Comparison of simple potential functions for simulating liquid water," *The Journal of Chemical Physics*, vol. 79, no. 2, pp. 926–935, 1983.

[30] B. Hess, H. Bekker, H. J. Berendsen, and J. G. Fraaije, "Lincs: a linear constraint solver for molecular simulations," *Journal of Computational Chemistry*, vol. 18, no. 12, pp. 1463–1472, 1997.

[31] B. Hess, C. Kutzner, D. Van Der Spoel, and E. Lindahl, "Gromacs 4: Algorithms for highly efficient, load-balanced, and scalable molecular simulation," *Journal of chemical theory and computation*, vol. 4, no. 3, pp. 435–447, 2008.

[32] E. F. Pettersen, T. D. Goddard, C. C. Huang, G. S. Couch, D. M. Greenblatt, E. C. Meng, and T. E. Ferrin, "Ucsf chimera-a visualization system for exploratory research and analysis," *Journal of Computational Chemistry*, vol. 25, no. 13, pp. 1605–1612, 2004.

[33] M. P. Allen and D. J. Tildesley, *Computer simulation of liquids*. Oxford university press, 1989.

[34] D. Olson, W. Haag, and W. Borghard, "Use of water as a probe of zeolitic properties: interaction of water with HZSM-5," *Microporous and Mesoporous Materials*, vol. 35, pp. 435–446, 2000.

[35] C. E. Ramachandran, S. Chempath, L. J. Broadbelt, and R. Q. Snurr, "Water adsorption in hydrophobic nanopores: Monte carlo simulations of water in silicalite," *Microporous and mesoporous materials*, vol. 90, no. 1, pp. 293–298, 2006.

[36] S. Chen and R. Yang, "Theoretical basis for the potential theory adsorption isotherms. the dubinin-radushkevich and dubinin-astakhov equations," *Langmuir*, vol. 10, no. 11, pp. 4244–4249, 1994.

[37] F. Porcheron, P. Monson, and M. Thommes, "Modeling mercury porosimetry using statistical mechanics," *Langmuir*, vol. 20, no. 15, pp. 6482–6489, 2004.

[38] M. Nagao and T. Morimoto, "Differential heat of adsorption and entropy of water adsorbed on zinc oxide surface," *The Journal of Physical Chemistry*, vol. 73, no. 11, pp. 3809–3814, 1969.

[39] K. Zhang, R. P. Lively, J. D. Noel, M. E. Dose, B. A. McCool, R. R. Chance, and W. J. Koros, "Adsorption of water and ethanol in MFI-type zeolites," *Langmuir*, vol. 28, no. 23, pp. 8664–8673, 2012.

NOMENCLATURE

Symbol	Quantity	SI Unit
E_{DA}	D-A energy parameter	$Jmol^{-1}$
k_B	Boltzmann constant	$1.380 \cdot 10^{-23} JK^{-1}$
n_{DA}	D-A geometry parameter	–
N_A	Avogadro number	$6.022 \cdot 10^{23} mol^{-1}$
p	pressure	Pa
q	partial charge	C
t	time	s
T	temperature	K
σ	12-6 LJ parameter	m
ω	water uptake	–